Available online at www.sciencedirect.com
SCIENCE DIRECT®
Applied Thermal Engineering 24 (2004) 2207–2217
APPLIED THERMAL ENGINEERING
www.elsevier.com/locate/apthermeng

Thermoelectric cooler application in electronic cooling

Reiyu Chein *, Guanming Huang

Department of Mechanical Engineering, National Chung Hsing University, 250 Kuo-Kuang Rd., Taichung City 402, Taiwan, ROC

Received 5 July 2003; accepted 1 March 2004
Available online 9 April 2004

Abstract

This study addresses thermoelectric cooler (TEC) applications in the electronic cooling. The cold side temperature (T_c) and temperature difference between TEC cold and hot sides ($\Delta T = T_h - T_c$, T_h = temperature of hot side of TEC) were used as the parameters. The cooling capacity, junction temperature, coefficient of performance (COP) of TEC and the required heat sink thermal resistance at the TEC hot side were computed. The results indicated that the cooling capacity could be increased as T_c increased and ΔT was reduced. The maximum cooling capacity and chip junction temperature obtained were 207 W and 88 °C, respectively. The required heat sink thermal resistance on TEC hot side was 0.054 °C/W. Larger cooling capacity and higher COP could be obtained when the TEC was operated in the enforced regimes ($\Delta T < 0$). However, TEC performance was restricted by the T_c values and heat sink thermal resistance at the TEC hot side. A microchannel heat sink using water or air as the coolant was demonstrated to meet the low thermal heat sink resistance requirement for TEC operated at maximum cooling capacity conditions.

Keywords: Thermoelectric cooler; Electronic cooling; Enforced regimes; Microchannel heat sink

1. Introduction

Since the birth of electronic technology, the heat flux generation from electronic devices has increased and this trend is expected to continue. According to the International Technology Roadmap for Semiconductors [1], the predicted maximum power dissipation from a single chip package will be 170 W in the year 2008. Moreover, the allowable maximum junction temperature

* Corresponding author. Tel.: +886-4-22850462; fax: +886-4-22877170.
E-mail address: rychein@dragon.nchu.edu.tw (R. Chein).

1359-4311/$ - see front matter
doi:10.1016/j.applthermaleng.2004.03.001

Nomenclature

C_{pf}	specific heat of coolant, J/kg K
D_h	hydraulic diameter of microchannel, m
F	geometric factor of microchannel
G	geometric factor of thermoelectric element, m
h	heat transfer coefficient, W/m^2 K
I	electric current, A
I_{opt}	optimal electric current for maximum cooling capacity, A
K	thermal conductivity of thermoelectric element, W/m K
k_f	thermal conductivity of coolant, W/m K
k_{fin}	thermal conductivity of fin, W/m K
L_{hs}	length of microchannel heat sink, m
L_{ch}	depth of microchannel
N	number of pair of thermoelectric element
n	number of microchannel of heat sink
Nu	Nusselt number
Pow	coolant pumping power of microchannel heat sink, W
Q_p	power input to TEC
Q_c	heat rate at TEC cold side
Q_h	heat rate at TEC hot side
r	electric resistivity, Ω m
R_1	contact thermal resistance, K/W
R_2	heat sink thermal resistance, K/W
Re	Reynolds number based on hydraulic diameter
S	Seebeck coefficient, V/K
T_a	ambient temperature, K
T_c	TEC cold side temperature, K
T_j	chip junction temperature, K
T_h	TEC hot side temperature, K
u_m	averaged coolant velocity in microchannel, m
$\dot{V}$	coolant volumetric flow rate, m^3/s
W_{ch}	width of microchannel, m
W_{fin}	width of fin, m
W_{hs}	width of microchannel heat sink, m

Greek symbols

β	$= L_{ch}/W_{ch}$
λ	friction factor of microchannel
v	viscosity of coolant, kg/m s
ρ_f	density of coolant, kg/m^3
ΔT	$T_h - T_c$, K

will have to be held to less than 85 °C for reliable operation and increased electronic device lifespan. Passive cooling technologies, such as the microchannel sink with a liquid as the working fluid [2], liquid immersion cooling [3], and jet impingement [4] could be the solution to provide high heat flux dissipation. However, maintaining the junction temperature at 85 °C or even lower is a challenging problem for passive cooling techniques because of the working fluid limitations. Active cooling technology integrated with electronic devices is possibly the only solution that could satisfy both requirements. One of the active cooling technologies is refrigeration cooling. Due to the space limits in practical electronic device packaging, a refrigeration system must have a size compatible to that of a chip, substrate, or board. Therefore, the so-called miniature refrigeration system should be considered in electronic heat management applications.

Miniature refrigeration systems have received much attention since the pioneer work by Little [5,6]. The review paper by Pelan et al. [7] summarized several current and future miniature refrigeration cooling technologies for high power microelectronics. According to Pelan et al. [7], a miniature vapor compression refrigerator could be a future solution for electronic heat management. In such a refrigeration system, the maximum power dissipation rate and lowest temperature that could be attained are 350 W and 12 °C, respectively. The miniature vapor compression refrigerator principle is the same as that for a conventional sized refrigerator except that the size is reduced to the centi- or millimeter order. Currently a miniature vapor compression refrigerator is under development using MEMS technologies [8–10]. The main difficulty is the microscale compressor design and fabrication. The microcompressor is the essential component in the vapor compression refrigerator. Another possible candidate that might also fit the requirement is a miniscale capillary pump loop (CPL) [11]. Operating such a system is similar to the mesoscale vapor compression refrigerator except that the working fluid is driven by capillary pressure.

Both the miniature scale vapor compression refrigerator and CPL are not commercially available. The only commercially available miniature size refrigerator today is the thermoelectric cooler (TEC). The basic TEC operating principle can be found in thermodynamic textbooks [12]. According to the data provided by suppliers [13,14], the TEC might not satisfy future requirements for electronic cooling because of its low cooling capacity and coefficient of performance. However, it does have advantages such as high reliability, flexibility in packaging and integration, low weight and more importantly maintaining the junction temperature as low as required. These characteristics make the TEC a candidate for electronic cooling applications.

TEC performance depends on several operation parameters: the temperatures of the TEC cold and hot sides, thermal and electrical conductivities of TEC thermoelement, contact resistance between the TEC cold side and the device surface, thermal resistance of heat sink on the TEC hot side, and the applied electric current. These large operational parameters have allowed a variety of TEC applications. For example, in applications providing refrigerated spaces or in dehumidification processes, the TEC is used to provide an environment with a temperature lower than ambient. When the TEC operation is reversed, it becomes a power generator that is one of the important applications in thermoelectric modules [15,16]. A recent review on the present and potential applications for thermoelectric modules was provided by Riffat and Ma [17].

In electronic cooling applications, the TEC serves as a device for transporting heat from a surface that has a temperature higher than ambient. The purpose of TEC is to maintain the electronic device junction temperature below a safe temperature by pumping heat away from the electronic devices. Although TEC utilization in electronic cooling were demonstrated by Simmons

and Chu [18] and Pelan et al. [7], the design on the heat sink at the TEC hot side was not addressed in detail. In this study, heat sink thermal resistance requirement for high TEC performance is to be addressed. The special attention will be focused on the TEC operated under a condition in which TEC cold side temperature is lower than that of hot side.

2. Modeling

The thermal management schematic for incorporating a TEC into electronic cooling is shown in Fig. 1. The heat generated by the chip is designated as Q_c which is removed by the TEC while the chip is kept at a temperature of T_j. The TEC is in contact with the chip surface with the thermal resistance denoted as R_1. The temperatures at the hot and cold sides of the TEC are T_h and T_c, respectively. TEC operation requires an input power of Q_p. At the hot side, the total amount of heat that must be dissipated into the ambient environment at temperature T_a is Q_h. This heat is dissipated by employing a heat sink whose thermal resistance is denoted as R_2. By assuming constant thermal and electric properties of the thermoelectric material and optimized geometric factor of thermoelectric element, Q_c, Q_p, and the TEC coefficient of performance can be written as [7,12,18],

$$Q_c = 2N\left[SIT_c - \frac{1}{2}I^2\frac{r}{G} - KG\Delta T\right] \tag{1}$$

$$Q_p = 2N\left[I^2\frac{r}{G} + SI\Delta T\right] \tag{2}$$

$$\mathrm{COP} = \frac{Q_c}{Q_p} \tag{3}$$

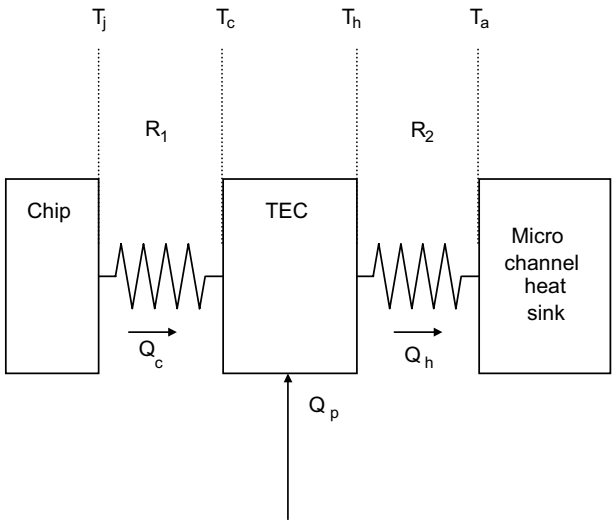

Fig. 1. Schematic diagram of the refrigeration cooling system.

The relationships between the temperatures at each location can also be derived from the energy balance,

$$T_j = T_c + Q_c R_1 \tag{4}$$

$$T_h = T_a + Q_h R_2 \tag{5}$$

From Eq. (1), the TEC cooling capacity is composed of three parts, i.e., the Peltier heat, Joulean heat loss and the conduction heat loss. The Peltier heat is proportional to I and T_c. The Joulean heating always decreases the cooling capacity and is proportional to the square of the electric current. The cooling capacity can be increased by either increasing T_c, decreasing ΔT, or operating the TEC in the so-called enforced regime with $\Delta T < 0$ [19]. For TEC operated in enforced regime, the heat conduction loss in Eq. (1) becomes a cooling capacity gain which also leads to reduce the input power as indicated in Eq. (2). Therefore, we might expect both the TEC cooling capacity and COP will be increased when it is operated in the enforced regime. We may view that TEC operated in the enforced regime as a heat pump that pumping heat away from hot body to cold body by input external power. From Eqs. (4) and (5), TEC performance also depends on the thermal resistances R_1 and R_2.

3. Results and discussion

3.1. System operation calculation

To carry out the TEC performance and heat sink design, the same commercially available TEC used in the study by Pelan et al. [7] was adopted in this study. The physical properties and thermoelectric element geometric factors were taken from Melcor [13]: $N = 31$, $S = 0.0002$ [$\mathrm{VK^{-1}}$], $r = 0.00001$ [$\Omega\,\mathrm{m}$], $K = 1.5$ [$\mathrm{W\,m^{-1}\,K^{-1}}$], $G = 0.01196$ [m].

The calculation procedure is shown in Fig. 2. Because the primary purpose of using a TEC is to maintain T_j at a designed value, the calculation starts from specifying T_c and ΔT. By knowing T_c and ΔT, we can compute the cooling capacity Q_c from Eq. (1) by inputting the electric current. From Q_c, the junction temperature T_j from Eq. (4) can be evaluated. After this, COP and the required R_2 can be found. The heat sink design to achieve the required R_2 will then be discussed.

In this study, T_c was chosen as 40, 60, and 80 °C and ΔT was chosen in the range of −20 to 50 °C. For these ranges of T_c and ΔT studied, optimum electric current I_{opt} for maximum Q_c can be found analytically or using the calculation procedures described in Fig. 2. In Table 1, TEC performances operated under maximum cooling capacity conditions for the ranges of T_c and ΔT studied were summarized. Several observations based on Table 1 can be made as follows:

(1) The maximum Q_c increased with decreasing in ΔT and increasing in T_c. The maximum cooling capacity obtained was 207 W when $\Delta T = -20$ °C and $T_c = 80$ °C. Although larger Q_c might be expected when ΔT is further reduced, this will be prohibited due to the heat sink performance limitation on the TEC hot side and will be discussed later.
(2) The TEC COP at maximum cooling rate is found to increase with decreasing in ΔT and T_c. Using the calculation procedure described in Fig. 2, it can be found that COP decreases

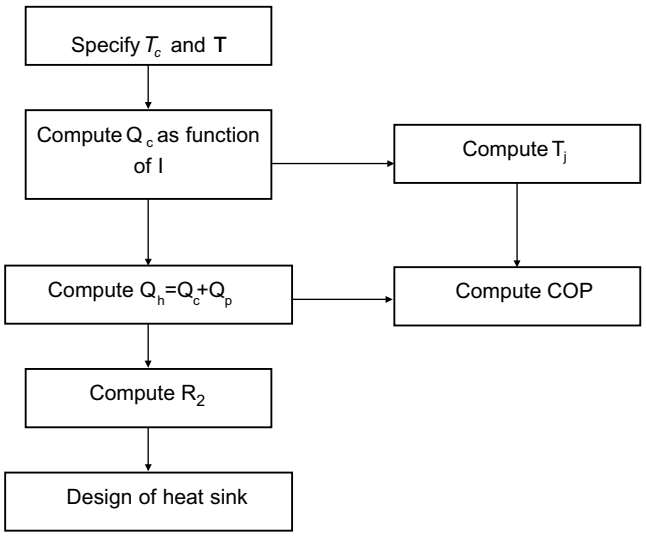

Fig. 2. Flow chart for the calculation procedure.

Table 1
Performance of TEC at maximum cooling capacity conditions

	$T_c = 40$ °C, $I_{opt} = 74.75$ A				$T_c = 60$ °C, $I_{opt} = 79.45$ A				$T_c = 80$ °C, $I_{opt} = 84.5$ A			
ΔT	Q_{max}	COP	T_j	R_2	Q_{max}	COP	T_j	R_2	Q_{max}	COP	T_j	R_2
−20	167.5	0.618	46.6		186.7	0.602	67.3	0.0201	207.0	0.591	88.1	0.054
−10	156.4	0.558	46.2		175.6	0.549	66.9	0.0404	195.9	0.540	87.7	0.072
0	145.3	0.502	45.7	0.023	164.5	0.499	66.5	0.0607	184.8	0.499	87.3	0.090
10	134.2	0.449	45.3	0.046	153.3	0.452	66.0	0.081	173.6	0.456	86.8	0.108
20	123.1	0.399	44.8	0.070	142.2	0.407	65.6	0.102	162.5	0.415	86.4	0.126
30	111.9	0.353	44.4	0.093	131.1	0.365	65.2	0.1230	151.4	0.377	86.0	0.145
40	100.8	0.309	44.0	0.117	119.9	0.325	64.7	0.1430	140.3	0.341	85.5	0.163
50	89.7	0.267	43.5	0.141	108.8	0.287	64.3	0.1640	129.2	0.306	85.1	0.181

monotonically with the increase of I when ΔT is less than 30 °C for the T_c range studied. For $\Delta T > 30$ °C, there appears an optimal I at which maximum COP can be obtained. However, these electric currents are too low to produce the desired cooling capacity. Enhancement of COP by operating TEC in the enforced regime is clearly shown in Table 1. Note that at maximum Q_c operations, all COP values drop below unity, even for TEC operating in enforced regime.

(3) The listed junction temperatures T_j in Table 1 were calculated by assuming $R_1 = 0.039$ °C/W [18]. As shown in Table 1, the differences between T_j and T_c are usually small provided that R_1 is not large. For a TEC operated at I_{opt} and $\Delta T = -20$ °C, T_j was found to be 46.6, 67.3, and 88 °C for $T_c = 40$, 60, and 80 °C, respectively. These are the maximum T_j for the chosen ranges of T_c and ΔT in the present study because T_j decreases with increasing ΔT. For the cases of

$T_c = 40$ and 60 °C, the resulting T_j are acceptable in electronic cooling applications because they are below the designed value of 85 °C. For the case of $T_c = 80$ °C, careful design to reduce R_1 is required to keep T_j below 85 °C.

(4) For the thermal heat sink thermal resistance at the TEC hot side, it is seen that R_2 decreases as ΔT decreased for the T_c range studied. This implies that good heat sink performance is required as ΔT is reduced, especially when TEC is operated in enforced regimes. In the case of $T_c = 40$ °C, R_2 cannot be defined when $\Delta T \leqq 0$ because T_h is lower than T_a. Note that when the TEC operation is at maximum cooling capacity conditions, the largest R_2 is 0.181 °C/W when $\Delta T = 50$ °C and $T_c = 80$ °C. It is impossible for a conventional heat sink to achieve such a low thermal resistance. The possibility of using a microchannel heat sink in electronic cooling applications to achieve the low heat sink thermal resistance requirement is discussed next.

3.2. Microchannel heat sink design

To reach the required heat sink thermal resistance value on the TEC hot side as shown in Table 1, we propose using a microchannel heat sink. Microchannel cooling has emerged in recent years as a highly effective means for dissipating large amounts of heat from a small heat transfer area. A microchannel heat sink typically contains a large number of parallel microchannel coolant passages ranging from 10 to 1000 μm. Air and liquid coolant such as water or fluorochemicals are two types of coolant favored in microchannel heat sinks. In this study, the microchannel heat sink size had the same size as the TEC and contacted directly to the TEC hot side. Fig. 3 shows the geometric configuration of the microchannel heat sink. The width and length of the microchannel heat sink are $L_{hs} \times W_{hs} = 5.5$ cm $\times$ 5.5 cm. The microchannel has a width of W_{ch} and a depth of L_{ch}. The wall that separates the channels is called the fin, with a width of W_{fin}. The base of the heat sink has a thickness of t_b. The microchannel heat sink top surface is assumed insulated. The heat sink performance is commonly measured by its thermal resistance defined as, [20,21]

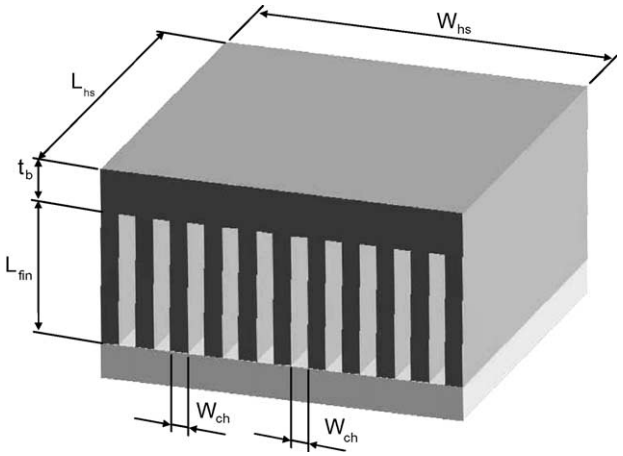

Fig. 3. Schematic of microchannel heat sink.

$$R_{th} = \frac{T_{w,max} - T_{f,in}}{Q_h/(W_{hs}L_{hs})} \tag{6}$$

where $T_{w,max}$ is the maximum heat sink surface temperature, and $T_{f,in}$ is the coolant inlet temperature. Based on a one-dimensional single-phase fluid flow, fin theory, and assuming uniform dissipated power distribution, the heat sink resistance can be expressed as,

$$R_{th} = R_{fin} + R_{cap} + R_{con} = \frac{1}{Nuk_f}\frac{1+\beta}{1+2\alpha\eta}\frac{2\alpha}{1+\alpha}W_{ch} + \frac{L_{hs}}{C_{pf}\mu_f}\frac{2}{Re}\frac{1+\beta}{1+\alpha} + \frac{t_b}{k_s} \tag{7}$$

R_{fin} represents the thermal resistance due to the heat conduction through the fins and convection from the fins into the coolant. R_{cap} is the capacitive resistance due to coolant heating as it absorbs energy passing through the channel, and R_{con} is the thermal resistance as the heat crosses the heat sink base plate. In Eq. (7), α and β are the microchannel aspect ratio and fin width to channel width ratio defined as,

$$\alpha = \frac{L_{ch}}{W_{ch}}, \quad \beta = \frac{W_{fin}}{W_{ch}} \tag{8}$$

C_{pf}, k_f and μ_f are the working fluid specific heat, thermal conductivity, and viscosity, respectively. k_s is the thermal conductivity of the microchannel heat sink material. η is the fin efficiency defined as [22],

$$\eta = \frac{\tanh(m\alpha)}{m\alpha}, \quad m = \sqrt{Nu\frac{1+\alpha}{\alpha\beta}\frac{k_f}{k_s}} \tag{9}$$

Re is the Reynolds number in the microchannel flow defined as,

$$Re = \frac{\rho_f \cdot u_m \cdot D_h}{\mu_f} \tag{10}$$

u_m is the mean fluid flow velocity in the microchannel given as,

$$u_m = \frac{\dot{V}}{nW_{ch}L_{ch}} \tag{11}$$

where $\dot{V}$ is the coolant volumetric flow rate and n is the number of channels in the microchannel heat sink given as,

$$n = \frac{W_{hs} - W_{fin}}{W_{ch} + W_{fin}} \tag{12}$$

In Eq. (10), D_h is the microchannel hydraulic diameter defined as,

$$D_h = \frac{2W_{ch}L_{ch}}{(W_{ch} + L_{ch})} \tag{13}$$

A power supply is required to drive the coolant in microchannel heat sink operation. The coolant required pumping power can be expressed as the product of the pressure drop across the heat sink Δp and volume flow rate $\dot{V}$, i.e.,

$$\mathrm{Pow} = \dot{V} \cdot \Delta p = \dot{V}\left(\lambda \frac{L_{\mathrm{hs}}}{D_{\mathrm{h}}} \rho \frac{u_{\mathrm{m}}^2}{2}\right) \tag{14}$$

where λ is the friction coefficient. In Eq. (9), the pressure drops at the channel inlet and exit were neglected because they are usually small compared to that in the microchannel. From Eqs. (2) and (14), in addition to the microchannel heat sink geometries, the Nusselt number Nu and friction coefficient λ are two important parameters for microchannel heat sink performance. Both Nu and λ depend on the flow regime and type of coolant used. We assumed the flow in the microchannel to be laminar and fully developed. Under such conditions, the most widely used Nu and λ correlations for pure fluid are given as [20,21]

$$Nu = 8.235(1 - 2.042\alpha^{-1} + 3.0853\alpha^{-2} - 2.4765\alpha^{-3} + 1.0578\alpha^{-4} - 0.1861\alpha^{-5}) \tag{15}$$

and

$$\lambda Re = 4(4.7 + 19.64G), \quad G = \frac{\left(\frac{1}{\alpha}\right)^2 + 1}{\left(\frac{1}{\alpha} + 1\right)^2} \tag{16}$$

$$Nu = \frac{hD_{\mathrm{h}}}{k_{\mathrm{f}}}, \quad Re = \frac{u_{\mathrm{m}} \cdot D_{\mathrm{h}}}{v_{\mathrm{f}}} \tag{17}$$

In Figs. 4 and 5, two examples of thermal resistances as function of the channel geometry are presented for both air-cooled and water-cooled microchannel heat sinks. The air-cooled heat sink material is copper with $L_{\mathrm{ch}} = 300$ mm and air pumping power of 10 W. The water-cooled microchannel heat sink is made of silicon with $L_{\mathrm{fin}} = 300$ μm and water pumping power of 4 W.

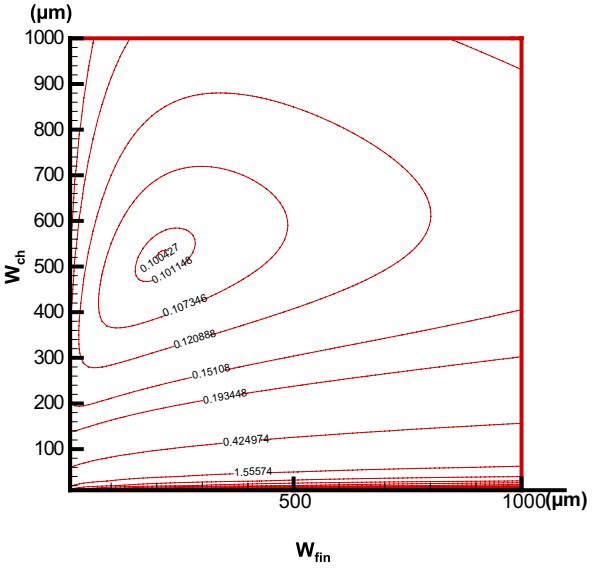

Fig. 4. Thermal resistance of an air-cooled microchannel heat sink as functions of the channel and fin widths. $L_{\mathrm{ch}} = 300$ mm, pumping power = 10 W.

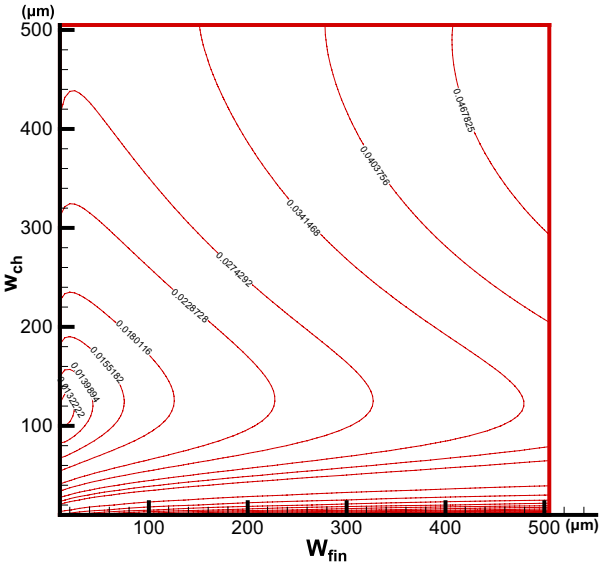

Fig. 5. Thermal resistance of a water-cooled microchannel heat sink as functions of the channel and fin widths. $L_{ch} = 300$ μm, pumping power = 4 W.

Because of higher thermal conductivity, liquid-cooled microchannel heat sink has lower thermal resistance comparing to that using air as coolant. Moreover, the bulk size of water-cooled microchannel heat sink is much smaller that the air-cooled one. Referring to Table 1, the smallest and largest heat sink thermal resistance required are 0.021 and 0.181 °C/W, respectively. In general, small R_2 is required when the TEC is operating in enforced regimes. From Figs. 4 and 5, the lowest R_2 that can be achieved are 0.1 and 0.013 °C/W for air-cooled and water-cooled microchannel heat sinks, respectively. Therefore, we conclude that a microchannel heat sink with liquid coolant must be employed to operate a TEC in enforced regimes. For a TEC operated with $\Delta T > 0$, an air-cooled microchannel sink is adequate by a wide range of microchannel geometric dimensions. Note that better microchannel heat sink performance can be obtained as coolant pumping power increases. However, this also increases of cost of operation.

4. Conclusion

A TEC electronic cooling application was investigated in this study. The conclusions from this study are as follows:

1. TEC cooling capacity and COP can be increased by increasing the TEC cold side temperature or decreasing temperature difference between the TEC hot and cold sides. The highest cooling capacity obtained in this study was as high as 207 W when the TEC was operated under electric current of 84.5 A, $T_c = 80$ °C, and $\Delta T = -20$ °C. The resultant junction temperature was 88 °C and the required heat sink thermal resistance was 0.054 °C/W. Although large cooling capacity

can be expected when a TEC is operated in an enforced regime, this operation is restricted by the cold side temperature and thermal resistance at the hot side.

2. Microchannel heat sinks must be employed to operate a TEC at maximum cooling capacity. The air-cooled microchannel heat sink was adequate for TEC operations with $\Delta T > 0$. For a TEC operated in enforced regimes, a water-cooled heat sink is required.

References

[1] The International Technology Roadmap for Semiconductors, Semiconductor Industry Association, 1999 edition.
[2] Z. Wen, C.K. Fah, The optimum thermal design of microchannel heat sinks, in: 1997 IEEE/CPMT Electronic Packaging Technology Conference, 1997, pp. 123–129.
[3] I. Mudawar, Assessment of high-heat-flux thermal management schemes, IEEE Trans. Compon. Pack. Manuf. Technol. 24 (2001) 122–141.
[4] C.H. Amon, J. Murthy, S.C. Yao, S. Narumanchi, C.F. Wu, C.C. Hsieh, MEMS-enabled thermal management of high-heat-flux devices EDIFICE: embedded droplets impingement for integrated cooling of electronics, Exp. Therm. Fluid Sci. 25 (2001) 231–242.
[5] W.A. Little, Micro-miniature refrigerator, Rev. Sci. Instrum. 55 (1984) 661–680.
[6] W.A. Little, Advances in Joule–Thomson cooling, Adv. Cryog. Eng. 35 (1990) 1305–1314.
[7] P. Phelan, V. Chiriac, T.Y. Lee, Current and future miniature refrigeration cooling technologies for high power microelectronics, in: 17th IEEE SEMI-THERM Symposium, 2001, pp. 158–167.
[8] T.A. Ameel, R.O. Warrington, R.S. Wegeng, M.K. Drost, Miniaturization technologies applied to energy systems, Energy Convers. Manage. 38 (1997) 969–982.
[9] N.S. Ashraf, H.C. Carter, K. Casey, L.C. Chow, S. Corban, M.K. Drost, A.J. Gumm, Z. Hao, A.Q. Hasan, J.S. Kapat, L. Kramer, M. Newton, K.B. Sundaram, J. Vaidya, C.C. Wong, K. Yerkes, Design and analysis of a meso-sale refrigerator, in: 1999 ASME International Mechanical Engineering Congress and Exposition, Nashhville, TN, USA, November 15–19, 1999, HTD 364-3, 1999, pp. 109–116.
[10] M.A. Shannon, M.L. Philpott, C.W. Bullard, D.J. Beebe, A.M. Jacobi, P.S. Hrnjak, T. Saif, N. Aluru, H. Sehitoglu, A. Rockett, J. Economy, Integrated mesoscopic cooler circuits (IMCCS), in: Proceedings of the ASME Advanced Energy Systems Division, AES, vol. 39, 1999, pp. 75–82.
[11] K. Pettigrew, B. Smith, K. Yerkes, C. Gamlen, D. Liepmann, Development and testing of planar, silicon mini-capillary pumped loop, in: 2001 ASME International Mechanical Engineering Congress and Exposition, New York, NY, USA, November 11–16, 2001.
[12] J.P. Holman, Thermodynamics, McGraw Hill, New York, 1980.
[13] Melcor homepage. http://www.melcor.com.
[14] Kryotherm homepage. http://www.kryothermusa.com.
[15] D.M. Rowe, G. Min, Evaluation of thermoelectric modules for power generation, J. Power Sources 73 (1998) 193–198.
[16] L. Chen, J. Gong, F. Sun, C. Wu, Effect of heat transfer on the performance of thermoelectric generators, Int. J. Therm. Sci. 41 (2002) 95–99.
[17] S.B. Riffat, X. Ma, Thermo-electrics: a review of present and potential applications, Appl. Therm. Eng. 23 (2003) 913–935.
[18] R.E. Simmons, R.C. Chu, Application of thermoelectric cooling to electronic equipment: a review and analysis, in: 16th IEEE SEMI-THERM Symposium, 2000, pp. 1–8.
[19] V.P. Babin, P.Y. Takhistov, Operation of thermoelectric module in enforced regime, in: 20th International Conference on Thermoelectrics, 2001, pp. 470–471.
[20] M.B. Kleiner, A. Kuhn, K. Haberger, High performance forced air cooling scheme employing microchannel heat exchangers, IEEE Trans. Compon. Pack. Manuf. Technol. 18 (1995) 795–804.
[21] R.W. Knight, J.S. Gooding, D.J. Hall, Optimal thermal design of forced convection heat sinks-analytical, J. Electron. Packaging 113 (1991) 313–321.
[22] A.F. Mills, Heat Transfer, 2nd ed., Prentice-Hall Inc., New Jersey, USA, 1999.